RELEVANCE OF COSMIC RADIATION EXPOSURE FOR HYPERSONIC FLIGHT

L. Koops, A. Sizmann
Bauhaus Luftfahrt e.V., Lyonel-Feininger-Str. 28, 80807 Munich, Germany

Abstract

In the present study, we quantitatively assess the relevance of cosmic radiation exposure for the conceptual design of future high-speed air transportation systems. To this end, for flight trajectories of representative point-to-point intercontinental hypersonic cruise missions, the effective radiation dose is calculated, which in general increases with cruising altitude, time spent at high latitudes and with traveled distance or flight time. Our results are compared to those for reference missions of present day airliners with significantly longer flight times as well as additional gas stops due to subsonic cruise velocities. We find that the trade-off between increased radiation levels at higher altitudes and shortened flight times results in a benefit of radiation dose reduction per traveled distance for trajectories with (partly) hypersonic cruise at Mach ~ 5 compared to those with purely subsonic cruise. We comment on the dependence of the results on the solar cycle as well as on the implications for route planning in the absence of possible radiation shielding solutions.

1 Introduction

A key driver for air transportation development is the reduction of journey time. Concepts of future hypersonic commercial aircraft promise point-to-point travel over the largest intercontinental distances in at most a few hours time [1]. However, to realize this goal, numerous technological challenges have yet to be overcome, one of which may be the protection of aircrew, passengers and aircraft electronics from enhanced levels of cosmic radiation.
The term *cosmic radiation* collectively comprises highly-energetic primary radiation, mainly protons and Helium nuclei, which originate from the sun as well as from outside of the solar system. It furthermore includes the cascades of secondary cosmic radiation, composed of an electromagnetic component – X-ray and Gamma-radiation – as well as of electrically charged and uncharged subatomic particles, created when the primaries enter the atmosphere and interact with its constituents. The intensity of the various radiation components, which move downwards in the atmosphere, is a function of their energy and depends mainly on altitude. In fact, from sea level to a maximum at $20 - 25$ km altitude, the radiation intensity grows roughly exponentially [14]. At current cruising altitudes of airliners, this already corresponds to 300 times larger radiation fluxes than on the ground. The exposure furthermore increases with latitude of the flight path such that polar routes are irradiated most [2].
In addition, during solar storms, the radiation intensity is temporarily boosted by a factor of 10 to 20 [4, 5]. Already for present cruising altitudes, the hazard to humans and risk of avionic failures during solar storms may cause significant economical penalties for airlines due to canceled flights or aircraft rerouting to lower altitudes and latitudes. While the latter option seems more troublesome for high-speed air transportation, there exists a trade-off between elevated radiation levels at higher altitudes and shortened travel times. A benefit of radiation dose reduction per traveled distance hence emerges in some high velocity range. However, a distance (and hence time) penalty may emerge for future high speed civil transportation aircraft as compared with subsonically flying commercial airliners. While the latter normally follow orthodromes (shortest connections between airports of departure and arrival), the 'sonic boom', or ground overpressure produced by supersonic flight adds requirements on possible flight routes and velocity profiles. In order to avoid on ground overpressures, future high speed civil transportation aircraft may only fly with super- or hypersonic velocities over regions of no or very low population density such as oceans and the north and south poles (flying over desert regions is also conceivable) [1]. The radiation dose, which future hypersonic commercial aircraft would be subject to on intercontinental flights, hence in general increases with cruising altitude, time spent at high latitudes and with traveled distance or flight time.
In the study at hand, it is our aim to evaluate the relevance of cosmic radiation exposure for concepts of future high-speed commercial transportation. To this end, in Sec. 2, we consider flight trajectories of representative hypersonic flight missions and define reference missions for long-range airliners at currently typical cruising altitudes. In order to quantify the hazard to humans associated with atmospheric cosmic radiation, as a first step, we analyze the dependence of the effective dose on altitude and latitude in Sec. 3.1. In Sec. 3.2, we parametrize the variation of latitude along the considered flight trajectories. We are then in a position to determine the effective dose rates along the different routes, which can be

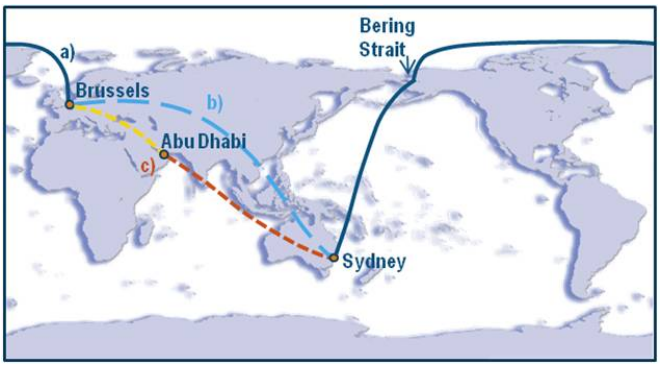

Figure 1: The three considered trajectories from Brussels to Sydney: a) hypersonic overflight of Bering Strait (solid), b) first portion of flight trajectory in eastern direction to Volgograd subsonic cruise, followed by hypersonic cruise to Sydney (dashed), and for reference c) subsonic cruise (dotted), with gas stop in Abu Dhabi.

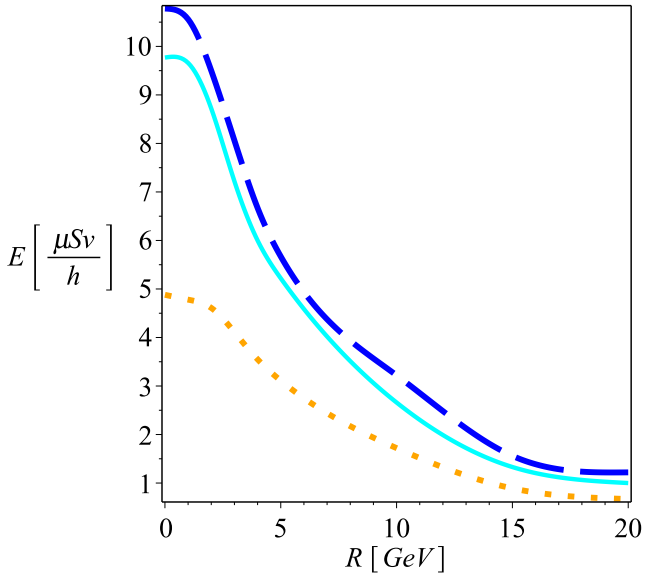

Figure 2: Effective dose rate as a function of cut-off rigidity R at flight altitudes of 28 km (solid) and 25 km (dashed) as typical for cruise at Mach ~ 5 and for reference at 10.7 km for cruise at Mach 0.85.

found in Sec.3.3. As a final outcome in Sec. 3.3, we analyze and compare the associated total effective doses. Eventually, in Sec.4, we summarize our results and conclude providing an outlook for ongoing and future work.

2 Definition of Missions

In the study at hand, we consider flight routes envisaged for long-distance commercial transport with Mach numbers ranging from 4 to 8 within a three-year project called LAPCAT (Long-Term Advanced Propulsion Concepts and Technologies), kicked-off by the European Commission (EC) in 2005 [1]. The baseline mission of LAPCAT is Brussels to Sydney, which could greatly benefit from hypersonic flight in terms of travel time savings compared to subsonic flight. In the following, we will consider three different flight trajectories, all of which with these airports of departure and arrival (cf. Fig. 1). The first two are chosen according to Ref. [1] and the last one is the reference mission:

a) In western direction, hypersonic cruise at Mach 5, overflight of Bering Strait, $D = 18,728$ km non-stop, total travel time 4.6 h.

b) In eastern direction along orthodrome, first portion of flight trajectory to Volgograd subsonic cruise, followed by hypersonic cruise at Mach 4.5 to Sydney, $D = 16,700$ km non-stop, total travel time 6.5 h.

c) Reference mission: in eastern direction subsonic flight, $D = 17,260$ km with gas stop in Abu Dhabi after $5,158$ km, total travel time 22.5 h including a 2 h gas stop.

In comparison, trajectory a) is the longest, but since it proceeds almost exclusively over water regions, it allows for hypersonic velocities during the very largest portion of flight.
Trajectory b) corresponds to a direct connection following the orthodrome. It should be noted that for LAPCAT this is only true up to some deviations to avoid some densely populated areas, adding about 200 km to the shortest great circle route [1]. However, since the deviations in latitude, and hence their impact on the effective dose along the trajectory, are small, they will be neglected in the present study. While the total distance traveled along trajectory b) is shorter than that along trajectory a), the population density along the route requires a significant portion of cruise up to Volgograd to be subsonic [1]. As a consequence, the total travel time is roughly 40% larger than in case a).
Finally, trajectory c), presently served by Ethiad by commercial subsonically flying aircraft, follows orthodromes respectively from Brussels to Abu Dhabi as well as from Abu Dhabi to Sydney. As concerns the time in the air, it is roughly a factor 4.5 longer than in case a) despite of the 8.5% larger distance traveled. Compared with case b), the time in the air is more than three times larger at comparable distance.

3 Radiation Exposure

3.1 Effective Dose Rate

The biological response to ionizing radiation varies with the type of particle or radiation as well as its energy and is furthermore specific to cell or tissue type. The so-called effective dose quantifies the radiation hazard by incorporating appropriate weighting factors for each type of radiation as well as for various organs and tissue of the human body [7].
By means of the parametric AIR (Atmospheric Ionizing Radiation) model and the physics-based HZETREN (High Charge and Energy Transport) code, in Ref. [9], the effective dose of atmospheric ionizing radiation during so-

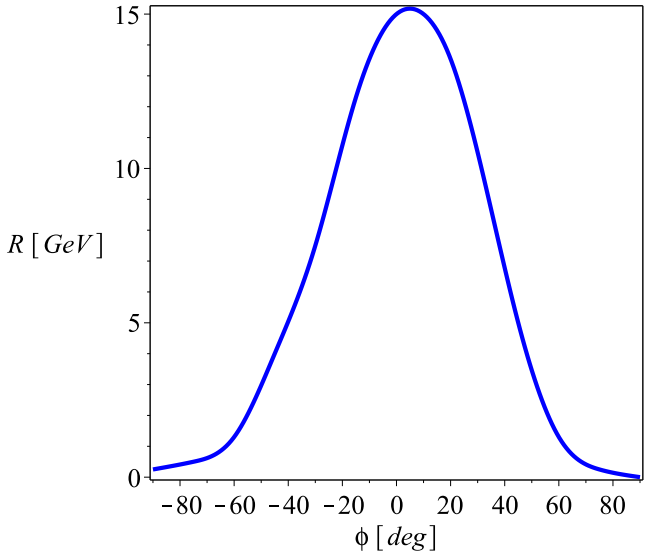

Figure 3: Cut-off rigidity as a function of latitude adopted from Shea and Smart [10, 11].

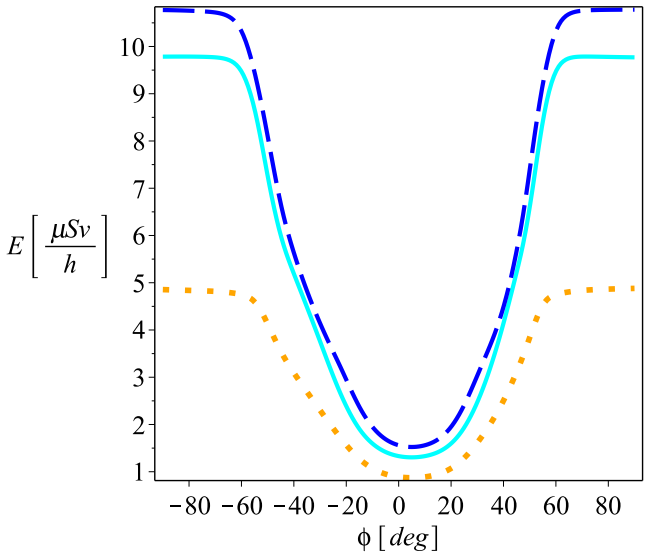

Figure 4: Calculated effective dose rate as a function of latitude at altitudes of 28 km (solid) and 25 km (dashed). Close to the poles the effective dose rate at 28 km and 25 km altitude is respectively up to 2.2 and 2 times larger than that at 10.7 km, while close to the equator it is larger by a factor of 1.8 and 1.5, respectively.

lar maximum is determined as a function of altitude for different geomagnetic cut-off rigidities R. The latter is defined to describe the propagation of charged energetic particles in the Earth's magnetic field and specifies the minimum momentum per charge a particle must have in order to reach a certain geographical location. In Fig. 2, we plot the effective dose rate of atmospheric ionizing radiation from Galactic Cosmic Rays (GCR) for different possible cruising altitudes as a function of cut-off rigidity according to the data from Ref. [9][1].
One observes that the effective dose rate increases with altitude. It furthermore exhibits a maximum for low cut-off rigidities and goes to zero for large cut-off rigidities. The reason is that the geomagnetic field provides a form of shielding by deflecting the lower-energy charged particles back to space by means of the Lorentz force.
In Fig. 3 we plot the zonal-averaged vertical geomagnetic cut-off rigidities as a function of latitude according to Shea and Smart [10, 11]. It becomes apparent that the shielding effect of the Earth's magnetic field is most efficient at low latitudes, where R, the minimum momentum per charge required to reach that latitude, is largest. Since it is our aim to determine the effective dose rate along trajectories of varying geographical coordinates, we determine the effective dose rate as a function of latitude by the help of the data underlying Figs. 2 and 3. Our result is plotted in Fig. 4. As expected, the magnitude of the effective dose rate increases with altitude and, for fixed altitude, is maximal at high latitudes and minimal at the equator.

[1] Due to the availability of data in the range of altitudes required for the present analysis, the radiation exposure due to GCR is considered during solar maximum. It should, however, be noted that during solar minimum, the magnitude of the effective dose rate as well as its increase with altitude is somewhat larger as indicated e.g. by Ref. [8].

3.2 Variation of Latitude along Flight Routes

In order to determine the effective dose rate along the trajectories, we parametrize the latitude in terms of the respective geographical coordinates of departure and arrival, A(ϕ_D, λ_D) and B(ϕ_A, λ_A), the distance d traveled normalized to the Earth's radius $R_E \sim 6371$ km and converted to degree measure, $\tilde{d} = (d/R_E)(180°/\pi)$, as well as of the course angle ω,

$$\begin{aligned} \phi &= \arcsin\Big(\Lambda(\phi_D, \tilde{d}, \omega)\Big), \\ \Lambda(\phi_D, \tilde{d}, \omega) &= \sin(\phi_D)\cos(\tilde{d}) + \cos(\phi_D)\sin(\tilde{d})\cos(\omega), \\ \cos(\omega) &= \frac{\sin(\phi_A) - \sin(\phi_D)\cos(\zeta)}{\cos(\phi_D)\sin(\zeta)}, \\ \cos(\zeta) &= \sin(\phi_D)\sin(\phi_A) \\ &+ \cos(\phi_D)\cos(\phi_A)\cos(\lambda_A - \lambda_D), \end{aligned} \tag{1}$$

where ζ is the central angle of the shorter great circle connecting A and B with arc length $D = (R_E\zeta)(\pi/180°)$ and $0 \le d \le D$. In Fig. 5, we have plotted the variation of latitude with time t normalized to the total flight time T, which results from Eq. (1) for the three distinct flight routes from Brussels to Sydney (cf. Fig. 1). In case of trajectory a), the latitude increases linearly for about a third of the travel time, before it decreases linearly towards the latitude of arrival. Accordingly, about 35% of the flight route proceeds in the north polar area (north of 60°N), where the effective dose rate is maximal (cf. Fig. 4). Trajectory b) remains somewhat south, but close to the north polar region at almost constant latitude for about 60% of the total travel time. However, as soon as hypersonic cruise has started, the latitude decreases continuously towards the latitude of arrival.
In contrast, trajectory c) almost linearly decreases with

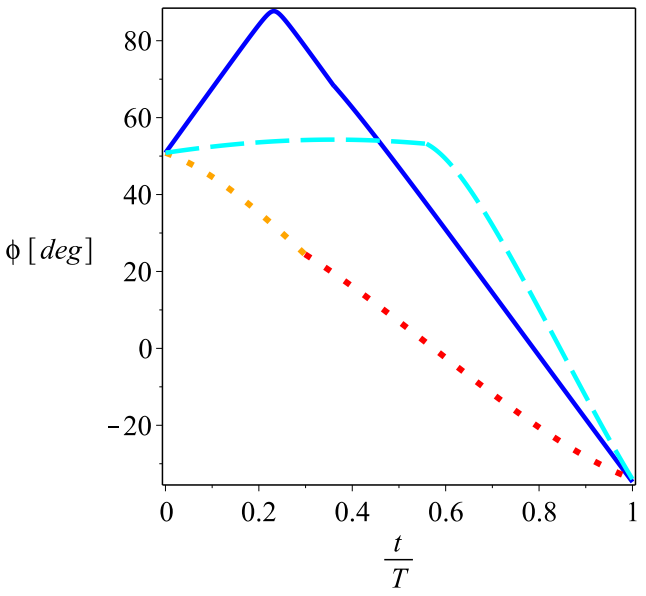

Figure 5: Variation of latitude as a function of time t normalized to total trip time T for three different routes connecting Brussels to Sydney: a) hypersonic overflight of Bering Strait (solid), b) first portion of flight trajectory in eastern direction to Volgograd subsonic cruise, followed by hypersonic cruise to Sydney (dashed), and for reference c) subsonic cruise (dotted), with gas stop in Abu Dhabi.

travel time such that on average, the effective dose rate is lowest. However, it should be kept in mind that in this case the significantly longer travel time enhances the contribution to the integrated effective dose as discussed in the next section.

For trajectory c), the reference case of a present day commercial aircraft flying subsonically with gas stop in Abu Dhabi, the average effective dose rate is considerably lower, since high latitudes are evaded. However, the flight time is significantly larger, which becomes apparent in Fig. 7.

The impact of flight time on the radiation exposure is taken into account by the integrated effective dose. In Figs. 8 and 9 it is respectively plotted as a function of traveled distance d and time t, where the total effective dose received on the trip emerges for $d = D$ and $t = T$, respectively. By comparison of Figs. 7 and 9, one observes that for trajectory a), its main contribution stems from the route segment lying in the north polar region. This is the case, even though roughly two thirds of the cruise time is spent at lower latitudes (cf. Fig. 5), since there a significantly smaller effective dose rate is received.

3.3 Effective Dose Accumulated Along Flight Routes

By means of the dependence of the effective dose rate on latitude plotted in Fig. 4 as well as the variation of latitude along the three considered flight trajectories shown in Fig. 5, we are now in a position to determine the effective dose rate along the flight routes. It is plotted in Figs. 6 and 7 as a function of traveled distance d and time t, respectively. Since for trajectories a) and c) the hypersonic and subsonic velocities respectively assumed during cruise are constant, d is proportional to t. This is, however, not the case for trajectory b), where roughly half of the cruise time proceeds subsonically and the other half hypersonically. But less than 20% of the total distance is covered within the subsonic regime.

In case of trajectory a), the effective dose rate assumes cruise altitudes of 25 km and 28 km, respectively, corresponding to the lower and upper cruise altitude of LAPTCAT for a cruise velocity of Mach 5. As expected from the discussion in the last section, while flying over the north polar region, the effective dose rate takes its maximal value, which is roughly 10% larger at 28 km altitude than at 25 km. Subsequently, the effective dose rate decreases to its minimal value at the equator to increase again until the final destination is reached.

In case of trajectory b), a jump in the effective dose rate is observed at about $d \sim 3,000$ km or equivalently $t \sim 3.2$ h, which is due to the increase in flight altitude and change of velocity from the subsonic to hypersonic regime. As concerns trajectory b), the main contribution stems from the segment of flight with subsonic cruise at the highest latitudes of flight (cf. Fig. 5). As can be seen in Fig. 7, the reason is that it makes up more than half of the total cruise time and – apart from a short period later on in hypersonic cruise – the effective dose rate takes its maximal value. In comparison to trajectory a), the growth of integrated effective dose with time in Fig. 9 is slower, in the end, however, reaches a similar level. The slower growth can be credited to the lower latitudes and hence significantly lower dose rate encountered during most of the flight, which is however encountered for a longer time due to the lower average flight velocity.

As a result, one observes that with a total of $32.5\,\mu$Sv, on trajectory c), the largest integrated effective dose is received on the reference mission (subsonic flight). It is followed by the total effective dose associated with trajectory a) at 28 km cruise altitude, which is with $22.7\,\mu$Sv, by roughly 60% lower than in the reference case. Finally, for trajectory b) the total effective dose is with $22.0\,\mu$Sv still somewhat lower than for trajectory a) at 28 km cruise altitude, but slightly larger than for trajectory a) at 25 km cruise altitude ($20.4\,\mu$Sv). However, compared to the reference case c), roughly 62% savings in effective dose result for trajectory b) with partly hypersonic cruise.

Tab. 1 in the appendix summarizes the results together with those for the average effective dose rate along the trajectories and respective values normalized to those on trajectory c). By definition, the normalized average effective dose rate $\frac{\bar{E}}{\bar{E}_{\mathrm{ref}}}$ is defined by the following equation,

$$\begin{aligned} \frac{E_{\mathrm{int}}}{E_{\mathrm{int,\,ref}}} &= \left(\frac{\bar{E}}{\bar{E}_{\mathrm{ref}}}\right)\left(\frac{T}{T_{\mathrm{ref}}}\right) \\ &= \left(\frac{\bar{E}}{\bar{E}_{\mathrm{ref}}}\right)\left(\frac{\bar{v}_{\mathrm{ref}}}{\bar{v}}\right)\left(\frac{D}{D_{\mathrm{ref}}}\right), \end{aligned} \qquad (2)$$

where in the last equality it has been used that $T = D/\bar{v}$, where $\bar{v}$ denotes the average velocity.

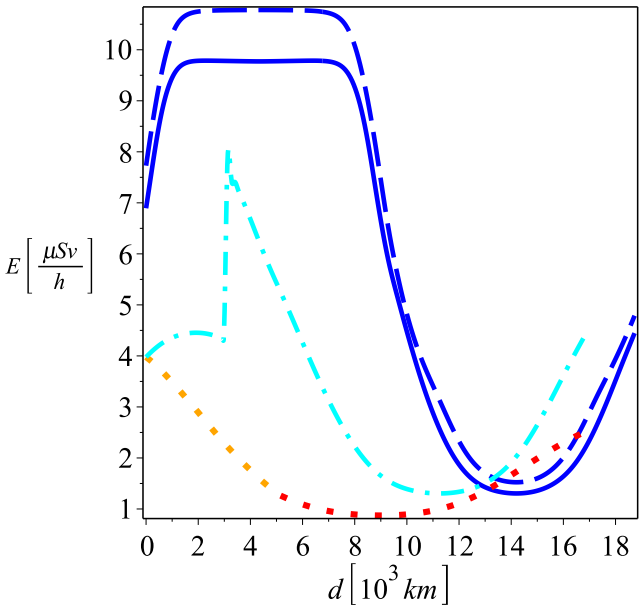

Figure 6: Effective dose rate as a function of distance d traveled along the three different flight routes from Brussels to Sydney: trajectory a) at cruise altitudes of 25 km (solid) and 28 km (dashed), respectively, trajectory b) (dash-dotted) and trajectory c) (dotted).

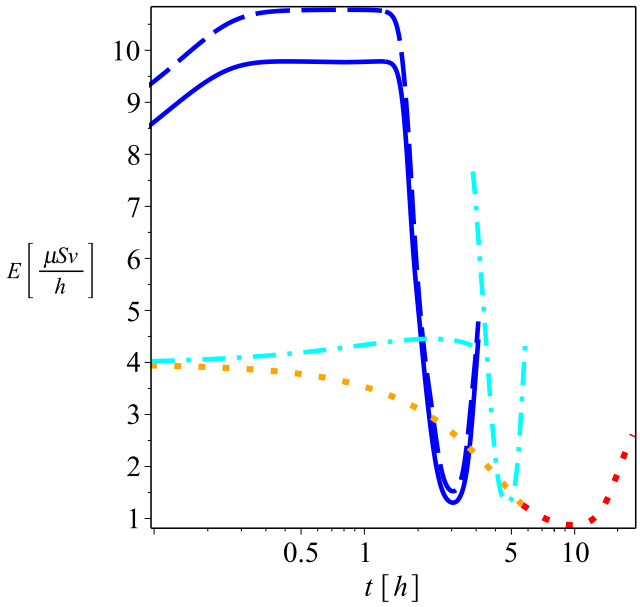

Figure 7: Effective dose rate as a function of time t traveled along the three different flight routes from Brussels to Sydney: trajectory a) with cruise altitudes of 25 km (solid) and 28 km (dashed), respectively, trajectory b) (dash-dotted) and trajectory c) (dotted).

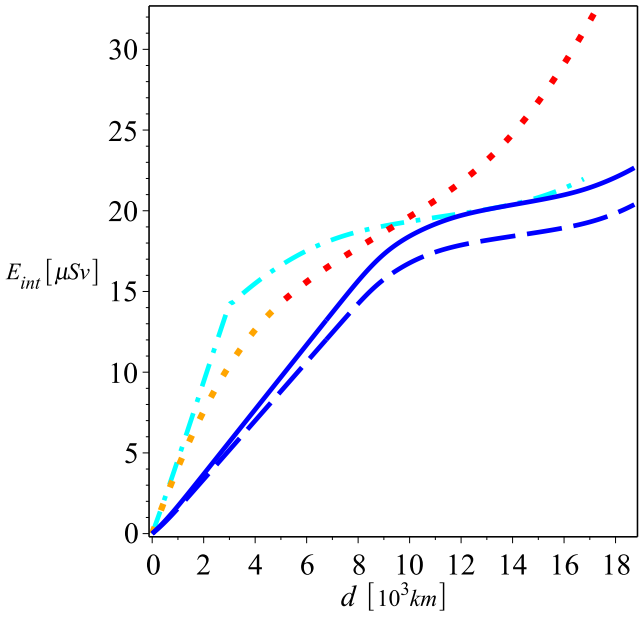

Figure 8: Integrated effective dose up to a distance d traveled along the three different flight trajectories from Brussels to Sydney: trajectory a) with cruise altitude of 25 km (solid) and 28 km (dashed), respectively, trajectory b) (dash-dotted) and trajectory c) (dotted).

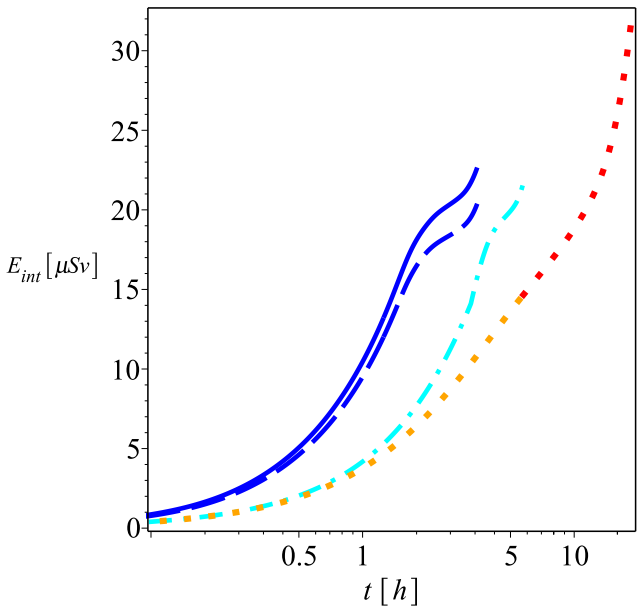

Figure 9: Integrated effective dose up to a time t traveled along the three different flight trajectories with flight time T from Brussels to Sydney: trajectory a) with cruise altitudes of 25 km (solid) and 28 km (dashed), respectively, trajectory b) (dash-dotted) and trajectory c) (dotted).

From Eq. (2) and Tab. 1 the reason becomes apparent for the larger total effective dose received on the reference mission compared to the (partly) hypersonic ones: the increase in average effective dose rate at higher altitudes is not large enough to overcompensate for the considerable decrease in flight time. The latter results from the increase in average velocity, while the respective distance penalty and benefit of the over-water-trajectory a) and the direct route b) with $D/D_{\mathrm{ref}} = 1.09$ and 0.97, respectively, are fairly insignificant for the result.
It is interesting to note that according to Fig. 8, at a distance of roughly $10,000$ km traveled along the three different routes, comparable integrated effective doses are received. The reason is that the reference mission has the benefit of receiving the lowest effective dose rates by evading high latitudes, which is in particular in contrast to trajectory a). Accordingly, the average effective dose rate along the first $10,000$ km of the route is low enough for the reference mission to (almost) compensate for the larger travel time in comparison to mission a) and b). However, since for the remaining part of all routes, higher latitudes are evaded, the effective dose rates of all missions are closer together (cf. Fig. 6), leading to the result for the total effective dose described above.
In conclusion, it should be noted that the reduction in total effective dose due to higher cruise velocities would not apply to flight crews with a fixed number of block hours on the route Brussels to Sydney as compared with the same number of hours on the reference trajectory at subsonic velocities. Here, for 500 h and 700 h block hours, flight crews would respectively receive up to 2.5 mSv and 3.5 mSv on trajectory a) and 1.7 mSv and 2.4 mS on trajectory b). On the reference route c) (subsonic flight), the total dose would respectively only amount to 0.8 mSv and 1.1 mSv. Compared with the annual allowable limit for the general public, which is 1 mSv [6, 7], the values for the (partly) hypersonic trajectories appear fairly high. However, classified as radiation workers, for aircrews an occupational dose limit of 20 mSv per year (averaged over 5 years) applies [6]. It should be noted that in particular during solar storms, but also during solar minimum the corresponding values are expected to be (significantly) larger. In order to stay within allowable limits, during solar storms the trajectories with (partly) hypersonic cruise at high altitudes could presumably not be served.

4 Conclusions and Outlook

In the present study, we investigated the relevance of cosmic radiation exposure for concepts of future high-speed commercial air transportation. To this end, we considered flight routes of the baseline mission Brussels to Sydney envisaged within the EC project LAPCAT (Long-Term Advanced Propulsion Concepts and Technologies) for a Mach ~ 5 aircraft [1]. Furthermore, we defined a reference mission for the same route served by present day subsonic commercial aircraft with a gas stop in Abu Dhabi.
To quantify the radiation hazard to humans, we analyzed the dependence of the effective dose rate both on altitude and on latitude. As a next step, we parametrized the variation of latitude along the respective flight trajectories, in order to determine the total effective dose that would be received on the different flight trajectories.
As a key result, we showed that there exists a trade-off between the increase in effective dose rate with flight altitude and the reduction in travel time resulting from (partly) hypersonic cruise in comparison to subsonic cruise. This trade-off originates from the dependence of the total effective dose along the trajectories both on the average effective dose rate along the routes and on travel time. However, since the occurrence of the 'sonic boom', or ground overpressures restricts hypersonic cruise to regions of non or low population density, considerable distance penalties may result for high speed air transportation. Yet, in the considered example case, the negative impact of both higher distance and altitude on the total effective dose are easily overbalanced by the positive influence of the reduction in cruise time. The latter is larger than a factor of 3 and 5 respectively, for partly and exclusively hypersonic cruise compared to that of the subsonic reference case. However, the increase in average effective dose rate along the (partly) hypersonic trajectories is only roughly a factor 2 and 4, respectively. Hence, for subsonic cruise at ~ 10.7 km altitude, with 32.5 μSv, $30-40\%$ larger effective dose rates resulted as compared with the (partly) hypersonic routes at higher cruise altitudes ($25-28$ km).
We found that besides flight altitude the routing itself plays a major role on the result. The reason is that due to the composition of the Earth's magnetic field, for example, at currently typical cruising altitudes of long-range airliners the effective dose rate in the polar regions takes values, which are roughly 2.5 times as large as those characteristic for Mach 5 aircraft (~ 25 km altitude) close to the equator. However, the subsonic flight trajectory from Brussels to Sydney via Abu Dhabi proceeds at fairly low latitudes, while the (partly) hypersonic trajectories pass (close to) the north polar region for a substantial fraction of the total cruise time, hence boosting the average effective dose rate. Accordingly, while the subsonic route receives relatively small dose rates compared to the distance traveled, this is not the case for the hypersonic routes. Yet, in total, owing to the significantly reduced cruise time, the effective dose is smaller.
When interpreting this result it should, however, be noted that the reduction in effective dose would apply for passengers, but not for flight crews with a fixed number of block hours on the routes from Brussels to Sydney as compared with the same number of hours on the reference trajectory at subsonic velocities. Here, e.g. for 500 or 700 block hours, flight crews would receive 0.8 mSv and 1.1 mSv, respectively, and hence roughly 2.5 or even 3.5 times the effective dose on the trajectories with (partly) hypersonic cruise in comparison to that on the reference trajectory with subsonic cruise.
It should furthermore be noted that due to the availability of data, in the present study, the exposure to atmo-

spheric ionizing radiation from GCR was investigated during solar maximum. However, during solar minimum, the magnitude of the associated effective dose rate as well as its increase with altitude is somewhat larger as, for example, indicated by Ref. [8]. Accordingly, during solar minimum, the effective dose of radiation from GCR received on the trajectories with (partly) hypersonic cruise are expected to be closer to that on the reference trajectory with subsonic cruise than during solar maximum.
In ongoing works [14], the impact of cosmic radiation exposure in particular on route planning of hypersonic flight is investigated for various conditions during the 11-year solar cycle, especially during solar storms, where radiation levels are dramatically elevated for short periods of time. As indicated, the impact of latitude on the effective dose of hypersonic flight at high altitudes can be quite significant and should hence be carefully considered in route planning. In particular, while present day aircraft may be rerouted to lower latitudes and altitudes during solar storms, this option is problematic for hypersonic missions. Hence, possible solutions for radiation shielding for hypersonic flight may be considered [12, 13, 15], in particular, options naturally arising for hydrogen-powered aircraft. As was shown in previous works [12], liquid hydrogen as a longterm alternative fuel allows for substantial co-benefits in radiation shielding.

References

[1] Steelant J. et al., *Long-Term Advanced Propulsion Concepts and Technologies (LAPCAT)*. European Commission, 6th Framework, Final Activity Report, AST4-CT-2005-012282, 2008.

[2] Holmes-Siedle, A., Adams, L.. *Handbook of radiation effects*. Oxford, 2002.

[3] European Commission, *Cosmic Radiation Exposure of Aircraft Crew*, Radiation Protection 140, Final Report of EURADOS WG 5, 2004.

[4] Newcome, L. R., “Impact of Solar Storms on High Altitude Long Endurance Unmanned Aircraft and Airship Design and Operations”, *Aeronaut. J.*, Vol. 110, No. 1111, pp. 623-626, 2006.

[5] Bentley, R. D. et al., “Monitoring Cosmic Radiation on Aircraft”, *Proceedings of the Second Solar Cycle and Space Weather Euroconference*. 2002.

[6] International Commission on Radiological Protection, “ICRP Publication 60 – The 1990 Recommendations of the International Commission on Radiological Protection”, *Ann. ICRP*, Vol. 21, Nos. 1-3, 1991.

[7] International Commission on Radiological Protection, “ICRP Publication 103 – The 2007 Recommendations of the International Commission on Radiological Protection”, *Ann. ICRP*, Vol. 37, Nos. 2-4, 2007.

[8] Sauer, H. H., "Notes on the Natural Radiation Hazard at Aircraft Altitudes", http://www.swpc.noaa.gov/info/RadHaz.html, 2007.

[9] Mertens, Christopher J. et al., “Atmospheric Ionizing Radiation from Galactic and Solar Cosmic Rays”, *Current Topics in Ionizing Radiation Research*, Vol. 1104, pp. 978-953, 2011.

[10] Shea, M. A., Smart, D. F., “Magnetospheric Models and Trajectory Computation”, *Space Science Reviews*, Vol. 93, pp. 305-333, 2000.

[11] Shea, M. A., Smart, D. F., “A Comparison of the Tsyganeko Model Predicted and Measured Cutoff Latitudes”, *Adv. Space Res.*, Vol. 28, pp. 1733-1738, 2001.

[12] Schrempp, L., Sizmann, A., “Shielding Cosmic Radiation in Air Traffic”, *28th Congress of the International Council of the Aeronautical Sciences, Brisbane, Australia*. Paper ICAS 2012-9.6.4, 2012.

[13] Schrempp-Koops, L., “Size Effects on the Efficiency of Neutron Shielding – a Full-Range Analysis”, *Int. J. Nanosci.*. Vol. 12, Iss. 3, 2013.

[14] Koops, L., Sizmann, A., work in preparation.

[15] Koops, L., work in preparation.

APPENDIX

Table 1: Comparison of average effective dose rate, cruise times and total effective dose for different trajectories from Brussels to Sydney.

Trajectory	$\bar{E}$ [$\frac{\mu\mathrm{Sv}}{\mathrm{h}}$]	$\frac{\bar{E}}{\bar{E}_{\mathrm{ref}}}$	T_c [h]	$\frac{T_c}{T_{c,\,\mathrm{ref}}}$	$\bar{E}_{\mathrm{int}}$ [μSv]	$\frac{\bar{E}_{\mathrm{int}}}{\bar{E}_{\mathrm{int,\,ref}}}$
a)	5.9^{a}-6.5^{b}	3.5^{a}-3.8^{b}	3.5	$(5.4)^{-1}$	20.4^{a}-22.7^{b}	0.6^{a}-0.7^{b}
b)	3.8	2.2	5.8	$(3.2)^{-1}$	22.0	0.7
c)	1.7	1	18.9	1	32.5	1

[a] At 25 km altitude

[b] At 28 km altitude